

# Probing temporal evolution of extreme ultraviolet assisted contamination on Ru mirror by x-ray photoelectron spectroscopy

A. Al-Ajlony, A. Kanjilal, M. Catalfano, M. Fields, S. S. Harilal,<sup>a)</sup> and A. Hassanein  
Center for Materials Under Extreme Environment, School of Nuclear Engineering, Purdue University,  
West Lafayette, Indiana 47907

B. Rice  
SEMATECH Inc., Albany, New York 12203

(Received 7 October 2011; accepted 4 January 2012; published 1 February 2012)

Extreme ultraviolet (EUV) radiation mediated carbon contamination and oxidation of the Ru mirror surface, and the corresponding impact on reflectivity were studied. In particular, time-dependent systematic decrease in EUV reflectivity with a 13.5 nm wavelength of light in high vacuum atmosphere was recorded and correlated with the change in chemical composition on the Ru surface as derived from *in situ* x-ray photoelectron spectroscopy (XPS). The contamination on Ru surface is caused by residual impurities of the test chamber. The recorded XPS spectra show a sudden increase in carbon concentration in the first 1 h followed by a slow but linear growth in the presence of EUV radiation. Further analyses show a slight increase in Ru oxide, whereas the concentration of water molecules decreases continuously. Moreover, the carbon monoxide level at the surface was stabilized after initial increase in concentration for an hour. The impact of water molecules and the accumulation of carbon atoms on the Ru surface are discussed in details. © 2012 American Vacuum Society. [DOI: 10.1116/1.3680122]

## I. INTRODUCTION

Extreme ultraviolet lithography (EUVL) is the leading candidate method for the production of next generation electronic devices with feature sizes down to 22 nm.<sup>1,2</sup> One of the advantages of this technique is the requirement of masks with feature sizes 4–5 times larger than that of the actual feature size of the products, whereas most other next generation lithography processes require  $1 \times$  membrane masks.<sup>1</sup> Although the development of the EUVL is advanced in wide steps during the last decade, many challenges still need to be overcome for commercial applications. Some of these challenges include the availability of reliable high power and clean extreme ultraviolet (EUV) source, and the long lifetime of the optics and masks. The EUV light requires special reflective optics rather than lenses as used in traditional optical lithography<sup>3</sup> due to high absorption of EUV photons when passing through any transparent materials and hence the entire system should be maintained in high vacuum condition. At present, 13.5 nm is selected as the wavelength of EUVL because of the existence of Mo/Si multilayer mirror (MLM), which reflects 13.5 nm with 2% bandwidth.<sup>4</sup>

The proposed EUVL system uses several MLMs for collecting and transferring the 13.5 nm light from plasma source to the mask and then to target wafer.<sup>5</sup> However, Mo/Si MLM shows a very poor chemical stability. Avoiding oxidation of the top Si layer under EUV exposure is vital for improving MLM's lifetime, and usage of thin capping layer is suggested to overcome this issue.<sup>3</sup> Among different elements,<sup>6</sup> Ru is considered one of the best capping materials to improve the lifetime of the Mo/Si multilayer stack<sup>1–3</sup> due to its optical properties (high transmission coefficient at

13.5 nm) and high tolerance to contaminants, even in corrosive environments.<sup>7</sup> However, thin Ru capping layer is also not free from contamination under EUV exposure, where the accumulation of free carbon atoms on Ru surfaces via dissociation of hydrocarbons<sup>8</sup> and the oxidation of the near surface atomic layers of Ru eventually lead to the degradation of the EUV reflectivity.<sup>9–11</sup>

EUV induced carbon contamination is one of the basic problems that limits the lifetime of EUV optics to significantly lower than the industrial target of 30 000 h. In previous studies, hydrocarbons have been injected into the test chamber from an external source for investigating carbon accumulation on the Ru mirror surface either during EUV exposure or by low energy electron bombardment.<sup>9,11,12</sup> Hard baking is not a feasible option for EUVL vacuum chamber from technological standpoints to avoid degradation of the EUV optics,<sup>13</sup> especially the quality of the interfaces of Mo/Si MLMs. The heating of such MLMs can initiate interlayer mixing, including the interface between the top Si and capping Ru layers, leading to the overall degradation in reflectivity.<sup>14</sup>

In this investigation we studied the effect of EUV induced carbon contamination and oxidation of Ru mirror surfaces in a high vacuum atmosphere. The real-time contamination caused by native hydrocarbons in the chamber is studied using *in situ* x-ray photoelectron spectroscopy (XPS) and correlated with systematic decrease in EUV reflectivity (EUVR). The corresponding change in EUVR will further be addressed on the ground of the observed chemical behavior of the Ru mirror surfaces.

## II. EXPERIMENTAL DETAILS

A 50-nm-thick Ru layer deposited on a 4 in. *p*-type Si (100) wafer was initially diced into several pieces with an

<sup>a)</sup>Electronic mail: hari@purdue.edu

average area of  $1 \times 1 \text{ cm}^2$ . The samples were sputter cleaned by  $2 \text{ keV Ar}^+$  for 15 min (beam current of  $\sim 590 \text{ nA}$ ) in a mildly baked ultra high vacuum (UHV) chamber (base pressure  $\sim 1.4 \times 10^{-8} \text{ Torr}$ ) at the materials characterization laboratory IMPACT at Purdue University.<sup>15</sup> This UHV system is equipped with a suite of *in situ* diagnostic tools for surface analysis including XPS, EUV photoelectron spectroscopy, Auger electron spectroscopy, ion scattering spectroscopy, and EUVR.<sup>15</sup> The XPS measurements were performed using an Al  $K\alpha$  radiation source ( $h\nu = 1486.6 \text{ eV}$ ), where photoelectrons emitted at  $45^\circ$  from the sample surface were analyzed with a PHOIBOS-100 hemispherical electron analyzer (energy resolution of  $0.8 \text{ eV}$ ). Calibration of binding energy (BE) scale with respect to the measured kinetic energy was made using the silver Fermi edge. High-resolution XPS spectra of the Ru mirrors surface were systematically recorded at various stages in presence of EUV radiation (EUV-ON) and absence of EUV radiation (EUV-OFF) to follow the change in surface chemical properties.

Grazing incidence EUVR of the Ru films has been investigated with the help of a Phoenix EUV source<sup>16</sup> that emits light in the range of  $12.5\text{--}15 \text{ nm}$  with a peak at  $\sim 13.5 \text{ nm}$  ( $92 \text{ eV}$ ), and two calibrated EUV photodiodes (PDs, International Radiation Detectors, Inc.). The estimated EUV total beam power reaching the sample surface is  $\sim 0.3 \mu\text{W}$ , whereas the total power of the photons with wavelength  $13.5 \text{ nm}$  (within 2% bandwidth)<sup>15,16</sup> is  $\sim 0.1 \mu\text{W}$ . The EUV beam spot size at the mirror surface was approximately  $7 \text{ mm}$ .

### III. RESULTS AND DISCUSSION

We performed XPS analysis for examining the surface properties of Ru during EUV exposure. Figure 1 exhibits the Ru  $3d$  region before sputter cleaning, immediately after sputtering and after exposing the cleaned surface to EUV radiation for 6 h. Clearly, the line shape of the Ru  $3d$  spin-orbit doublet has changed significantly after sputter cleaning, showing a dramatic increase of the Ru  $3d_{5/2}$ /Ru  $3d_{3/2}$  peak intensity. Close inspection reveals a shift in peak maximum of the Ru  $3d_{3/2}$  toward the higher BE region in presputtered sample. Similar phenomenon has previously been observed by depositing carbon on Ru surface<sup>17</sup>. It indicates C  $1s$  ( $284.6 \text{ eV}$ )<sup>18</sup> is dominating over the metallic Ru  $3d_{3/2}$  ( $284.2 \text{ eV}$ )<sup>17-19</sup> in the presputtered sample because of the accumulation of large amount of carbon. Although the spectral shape does not change much, the Ru  $3d_{5/2}$ /Ru  $3d_{3/2}$  peak intensity ratio is; however, found to be decreased after exposing the sputter cleaned Ru surface to the EUV radiation for 6 h compared to the one taken immediately after sputter cleaning (Fig. 1). The overlapping of the C  $1s$  and Ru  $3d$  peaks makes the fitting procedure complicated. A fixed FWHM, peak positions, line shape and  $3d_{5/2}$  to  $3d_{3/2}$  intensity ratio at  $\sim 1.5$ ,<sup>18</sup> all have been taken into account as peak fitting constraints for analyzing XPS spectra and following the evolution of concentration of the underlying components. From our analyses, we found that the Ru  $3d_{5/2}$  for pure metal (Ru<sup>0</sup>) and oxide phase of Ru (RuO<sub>2</sub>) are situated at  $280.1$  and  $280.8 \text{ eV}$ , respectively, whereas the Ru  $3d_{3/2}$  peak for

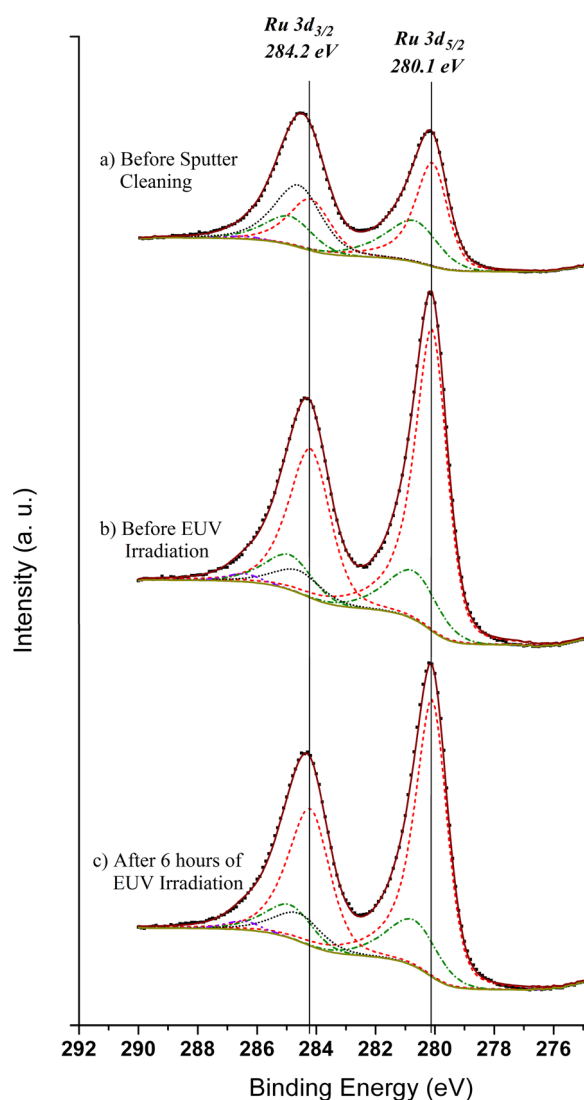


FIG. 1. (Color online) XPS spectra of Ru mirror Ru  $3d$ /C  $1s$  region before sputter cleaning (a), after sputter cleaning or before EUV irradiation (b) and after EUV radiated for 6 h (c). XPS spectra were fitted with asymmetrical peaks. The fitting components for Ru<sup>0</sup> peaking at  $284.2$  and  $280.1 \text{ eV}$  (dashed line), for RuO<sub>2</sub> peaking at  $284.9$  and  $280.8 \text{ eV}$  (dashed-dotted line), for C-C bonds situated at  $284.6 \text{ eV}$  (dotted line), and for C-O situated at  $286.5 \text{ eV}$  (dashed-dotted-dotted line).

Ru<sup>0</sup> and RuO<sub>2</sub> are at  $284.2$  and  $284.9 \text{ eV}$ , respectively.<sup>17-19</sup> Here we have considered RuO<sub>2</sub> as it is detected when fitting the O  $1s$  region (Fig. 2). The best fitting of the O  $1s$  region can be obtained using three components (Fig. 2) where the peaks at  $533.2$ ,  $531.7$ , and  $530.1 \text{ eV}$  represent the chemical states of oxygen in water (H<sub>2</sub>O) molecules, hydroxyl (OH) radicals and in RuO<sub>2</sub>, respectively. Going back to Fig. 1 again, we found that the C  $1s$  is situated at  $284.6 \text{ eV}$ ,<sup>18</sup> whereas the peak at  $286.5 \text{ eV}$  is believed to be associated with the oxide phase of carbon (i.e., C-O on top site<sup>20</sup>). As can be seen (Fig. 1), these peaks can reproduce well the experimental data.

In order to follow the chemical reaction dynamics on the Ru surface due to the adsorption and/or dissociation of gaseous molecules under EUV exposure in a systematic way, we have carried out EUVR and XPS studies at both Ru  $3d$  and

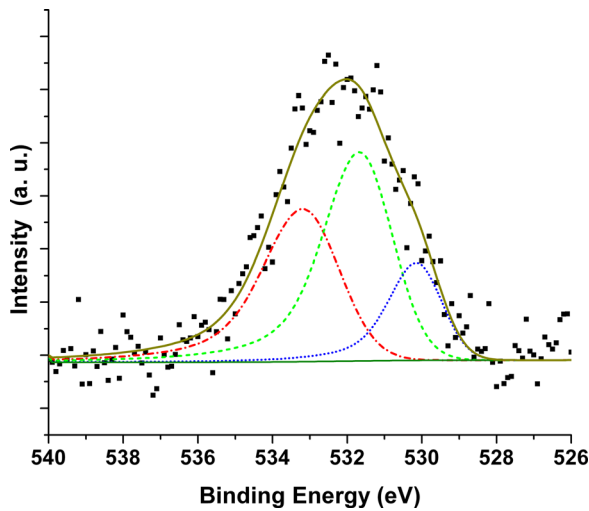


FIG. 2. (Color online) XPS spectrum of Ru mirror O 1s region right after sputtering. The fitting component for RuO<sub>2</sub> peaking at 530.1 (dotted line), for OH<sup>-</sup> peaking at 531.7 eV (dashed line), and for H<sub>2</sub>O peaking at 533.2 eV (dashed-dotted line).

O 1s regions with a 15 min interval. Detailed XPS analyses show a sudden increase in H<sub>2</sub>O on the Ru mirror surface after sputter cleaning and starting of the EUV irradiation (Fig. 3). It is important to note that the sputter cleaning process was stopped at the same moment when the EUV irradiation was started, and this moment is referred as “zero” time of EUV exposure. As discerned, H<sub>2</sub>O concentration is increased by 60% after ~30 min. We should mention here that the relative concentration signifies the ratio between the recorded data with EUV radiation time and the one just after sputter cleaning. During Ar<sup>+</sup> bombardment, water molecules are heavily dissociated into OH and H (H<sub>2</sub>O → OH + H), whereas two H atoms combine to form H<sub>2</sub> molecule and desorbs from the Ru surface. At the same time, the concentration of OH radicals on the Ru surface increases. Soon after sputter cleaning, not only the water molecules start adsorbing on the surface, but also the OH radicals start

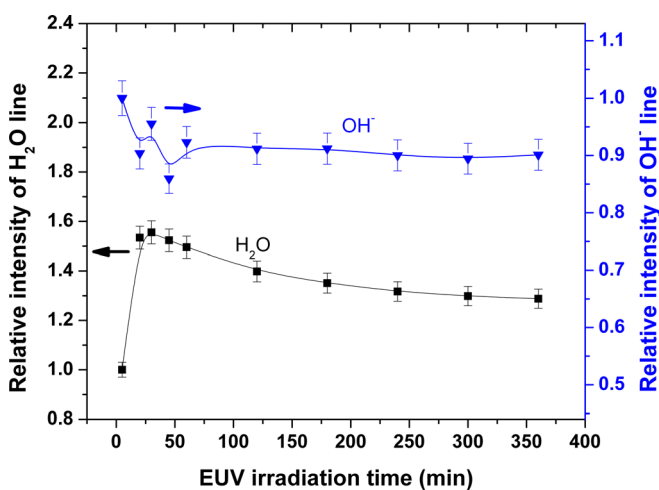


FIG. 3. (Color online) Changes in relative line intensity of H<sub>2</sub>O (left axes) and OH (right axes) with respect to EUV irradiation time.

interacting between each other to form H<sub>2</sub>O and free O atoms (2OH → H<sub>2</sub>O + O).<sup>13</sup> Hence, H<sub>2</sub>O concentration increases much faster than that of the decrease in OH. After 30 min, H<sub>2</sub>O concentration decreases slowly with increasing EUV dose without changing much in OH concentration. This observation clearly demonstrates that the dissociation of H<sub>2</sub>O takes place during EUV irradiation due to the interaction with secondary electrons (SEs) from the Ru surface,<sup>10,13</sup> whereas the subproduct OH is almost constant because of the fast reaction between the OH radicals. As the emission of SEs enhances with increasing molecular coverage on the metal surface,<sup>21</sup> the interaction with H<sub>2</sub>O will also increase gradually at the same time, and as a consequence more and more water molecules will be dissociated, in accordance with our results (Fig. 3). The free O atoms will react with both pure Ru atoms and deposited carbon on the Ru surface, and will be discussed in the following.

We found that during the first hour of the experiment the carbon was increasing dramatically to ~22%. After this initial jump, carbon concentration was found to increase linearly with a rate of 3%/h (Fig. 4). On the other hand, it was found that the Ru 3d<sub>5/2</sub> peak intensity is reduced almost exponentially in the first hour, followed by a linear trend in the remaining period as documented in Fig. 4. The rapid rise in carbon concentration in the first hour is most likely due to the dominance of direct adsorption of hydrocarbons over the accumulation of the carbon atoms alone via EUV-induced dissociation of adsorbed hydrocarbons<sup>8,13</sup> on the Ru surface, whereas the slow but linear increase in carbon concentration is mainly associated with the accumulation of free carbon atoms on the Ru surface after attaining a steady-state hydrocarbon coverage (will be justified by comparing the results without using EUV radiation in the following). In fact, it has been demonstrated previously that the carbon accumulation rate depends linearly on the dose in a steady state hydrocarbon coverage.<sup>11,17</sup> Going back to the trend of the Ru 3d<sub>5/2</sub>, the decrease in intensity in the first hour represents the adsorption of foreign species that include water molecules,

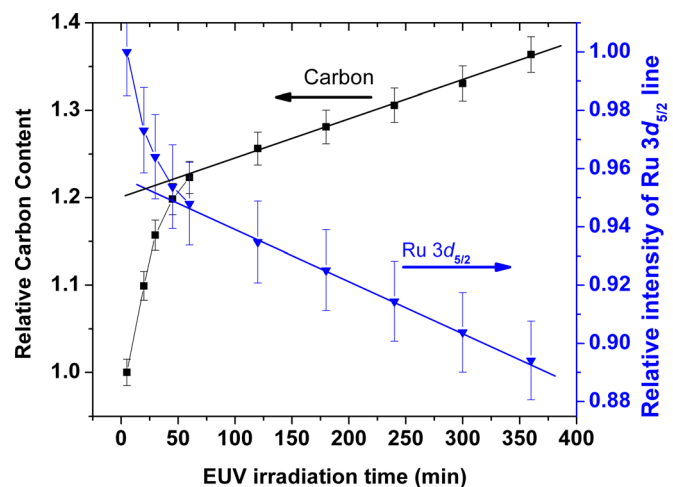


FIG. 4. (Color online) Changes in relative carbon line intensity (left axes) and Ru 3d<sub>5/2</sub> relative line intensity (right axes) with respect to EUV irradiation time.

hydrocarbons, and other gaseous contaminants on the Ru surface. The linear reduction of the Ru  $3d_{5/2}$  peak intensity that starts  $\sim 60$  min after EUV irradiation is most likely associated with the deposition of free carbon atoms on the Ru surface via decomposition of hydrocarbons during EUV exposure.<sup>17</sup> This is also consistent with the linear increase in intensity of the carbon line followed by parallel reduction in intensity of the adsorbed water molecules over the same period of time (see Fig. 4), suggesting that the carbon atoms are slowly covering the surface with a gradual suppression of the Ru signal.

For confirming the effect of adsorbents on the changes in surface chemical composition in the first hour of our experiment, another Ru mirror was sputter cleaned and scanned by XPS in 5 min intervals for an hour in the absence of EUV irradiation (Fig. 5). In this case carbon was found to increase by 25%, which is slightly higher than what we found with EUV irradiation within the first hour (Fig. 4), indicating that the initial rise in carbon concentration (Fig. 4) is not related to EUV assisted carbon deposition via decomposition of hydrocarbons alone. Instead, it confirms that the carbon accumulation during this time period is mainly related to those hydrocarbons that can be adsorbed immediately after reaching the Ru surface from the surrounding atmosphere.<sup>8</sup> It is worthwhile to note that when performing similar experiments with another sputter cleaned sample (not shown), the increase in carbon concentration was found to saturate after 1 h in the absence of EUV exposure. This phenomenon further confirms that the sputter cleaned Ru surface is stabilized after 1 h through adsorption of reactive hydrocarbons. Moreover, we found that the decrease in Ru  $3d_{5/2}$  peak intensity in the EUV-OFF case is  $\sim 5\%$  (Fig. 5), where the trend is similar to the case with EUV irradiation within the first hour (Fig. 4).

To estimate the EUV radiation-enhanced deposited carbon thickness, the linear behavior of the Ru  $3d_{5/2}$  line (in the time range between 60 and 360 min in Fig. 4) was used.<sup>17</sup> The calculation is based on an assumption of a uniform deposition of carbon in the form of graphite with a density<sup>22</sup>

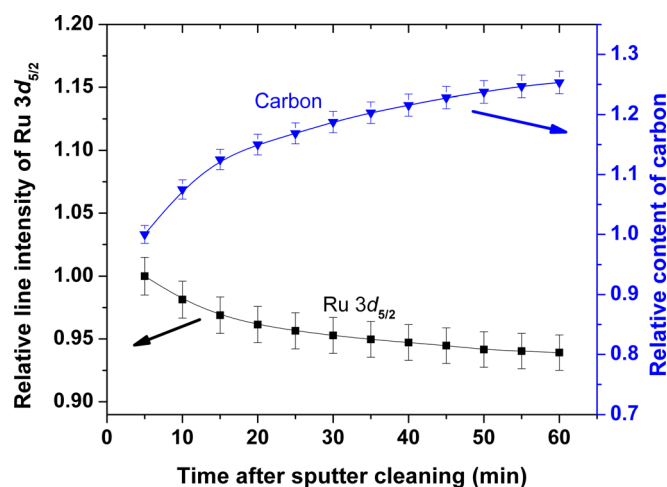


FIG. 5. (Color online) Changes in pure Ru  $3d_{5/2}$  relative line intensity (left axes) and relative carbon content (right axes) with respect to time after sputter cleaning in absence of EUV irradiation.

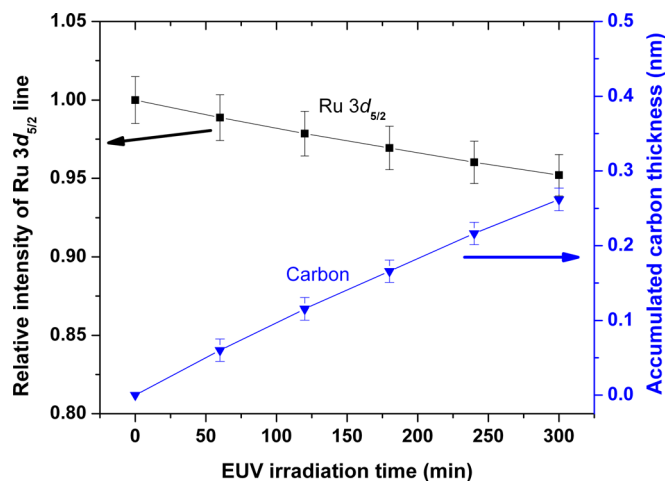


FIG. 6. (Color online) Changes in Ru  $3d_{5/2}$  relative line intensity (left axes) and accumulated carbon thickness (right axes) vs EUV irradiation time. The linear behavior of Ru  $3d_{5/2}$  line intensity was only considered, which is corresponded to the time window (60–360 min) of the original EUV irradiation time of this experiment.

of  $2.26 \text{ (g/cm}^3\text{)}$ . We use the attenuation equation<sup>17</sup> of Ru  $3d_{5/2}$  photoelectron signal:  $I = I_0 \exp(-d/\lambda \cos \theta)$  for this calculation where  $I$  is the Ru  $3d_{5/2}$  line intensity after carbon contamination,  $I_0$  is the initial Ru  $3d_{5/2}$  line intensity,  $d$  is the carbon thickness (nm),  $\lambda$  (i.e.,  $2.8 \text{ nm}^{-1}$  in our case)<sup>22</sup> is the mean free path of electrons when passing through a carbon (graphite) layer with  $1206.5 \text{ eV KE}$  [ $\text{KE} = h\nu - \text{BE}$ ,  $\text{BE} = 280.1 \text{ eV}$  (Ref. 18)], and  $\theta$  is the emission angle (i.e.,  $45^\circ$ ). The estimated carbon thickness is summarized in Fig. 6, showing a linear increase in thickness with a rate of  $\sim 0.54 \text{ \AA/h}$ .

In order to have a clear image of the surface chemical changes during EUV exposure, it is important to follow the Ru-oxide line (see Fig. 7). As can be seen,  $\text{RuO}_2$  is decreasing at a higher rate in the first hour followed by a slow rise in intensity up to 180 min. It decreases again after 180 min. Such a behavior of the  $\text{RuO}_2$  may be controlled by two

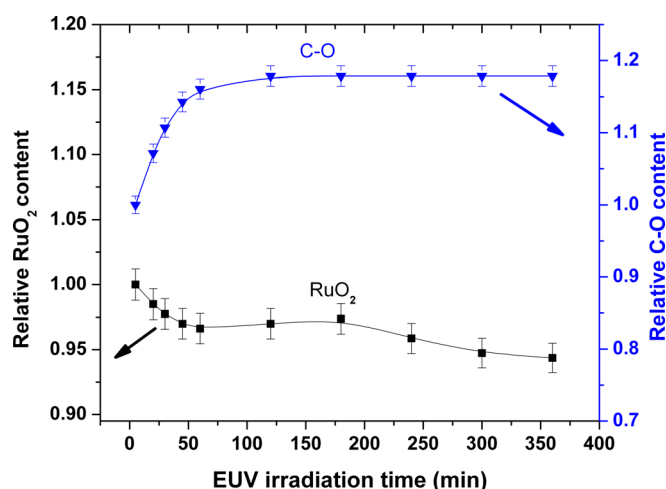


FIG. 7. (Color online) Changes in relative line intensity of  $\text{RuO}_2$  (left axes) and C-O (right axes) with respect to EUV irradiation time.

parallel mechanisms: The decrease in intensity of the RuO<sub>2</sub> line in the first hour is due to surface coverage by the gaseous molecules (adsorption) and free carbon atoms (dissociation), whereas the second mechanism is representing the increase in RuO<sub>2</sub> signal due to the oxidation of pure Ru atoms by free O atoms, which are created via EUV assisted dissociation of the H<sub>2</sub>O molecules on the top of the Ru surface (stated previously). In fact, attaining the saturation in Ru oxidation process gives the advantage to the first mechanism (surface coverage) to dictate the overall behavior of the RuO<sub>2</sub> behavior in the remaining time of the experiment. The reduction in intensity of the RuO<sub>2</sub> line after 180 min is basically associated with the gradual dominance of the second process (carbon deposition) over the first (adsorption). The saturation in RuO<sub>2</sub> at ~180 min can, therefore, be a transition from the oxidation of the surface Ru atoms to the accumulation of free carbon at the surface for protecting and/or isolating the underneath Ru atoms from further oxidation.<sup>9,23</sup> Also it is shown in Fig. 7 (right ordinate) that the carbon monoxide (C–O) line is also increasing fast in the first hour, and saturates after 120 min. The initial increase in C–O can be explained in terms of fast reaction of the adsorbed carbonaceous species with either water molecules or free O atoms (discussed previously). It seems that this process has reached a maximum after 120 min where a dynamic equilibrium between formation due to oxidation and dissociation due to EUV assisted breakage has attained and maintains a steady state in the rest of the EUV radiation time.

Further, in the EUV-OFF case water is increased by 60% in the first 30 min and it maintains a stable condition in the following hours (Fig. 8). Although similar 60% increment in water concentration is noticed in EUV-ON case, it decreases after 30 min (see Fig. 3) due to EUV assisted dissociation of water molecules. We should also point out that the intensity of the RuO<sub>2</sub> line is reduced by 8% in 60 min in the EUV-OFF case, whereas it has been decreased by 4% in the EUV-ON case. In fact, in any case

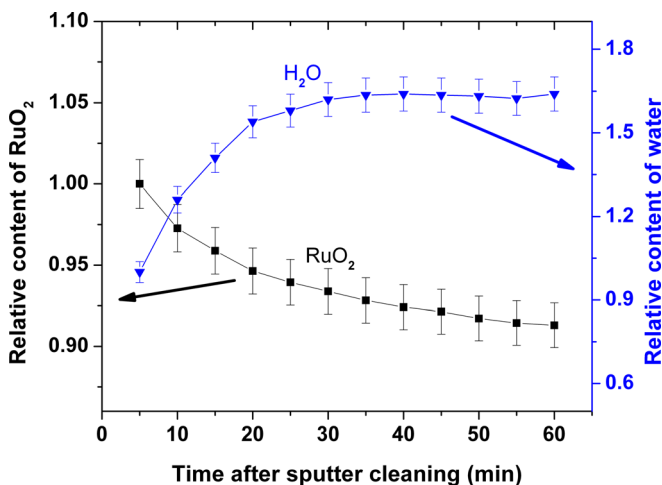


Fig. 8. (Color online) Changes in RuO<sub>2</sub> relative lines intensity (left axes) and relative water content (right axes) with respect to time after sputter cleaning in absence of EUV irradiation.

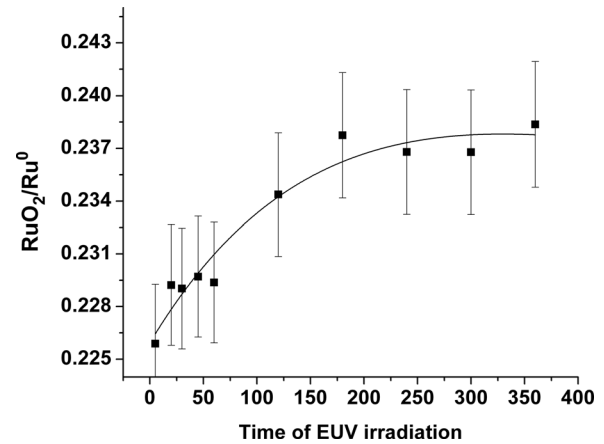


Fig. 9. Changes in the ratio of RuO<sub>2</sub> to Ru<sup>0</sup> line intensities with respect to EUV irradiation time in minutes.

the observed decrease is expected due to surface coverage via adsorption of foreign species. The surface coverage is mainly due to water molecules and carbon atoms, and they are found to be almost similar in both cases. Thus, the lower decrease in RuO<sub>2</sub> in the EUV-ON case supports our conclusion of a slight oxidation of Ru atoms caused by EUV assisted dissociation of water molecules, in good agreement with previous reports.<sup>5,13</sup> The changes in the ratio of RuO<sub>2</sub> to Ru<sup>0</sup> intensities with respect to EUV irradiation time is given in Fig. 9, which clearly shows oxidation is taking place during EUV irradiation.

Finally, the corresponding EUVR of the Ru surface at a grazing angle of ~15° was found to be reduced by 10% after 6 h of EUV radiation (Fig. 10). Based on our detailed analyses of the time-dependent variation of the surface chemical compositions, we can justify the observed change in EUVR in the light of surface contamination by carbon and slight oxidation of the top Ru layer via EUV-induced dissociation of residual hydrocarbons<sup>8</sup> and water vapor,<sup>10,13</sup> respectively, in our test chamber.

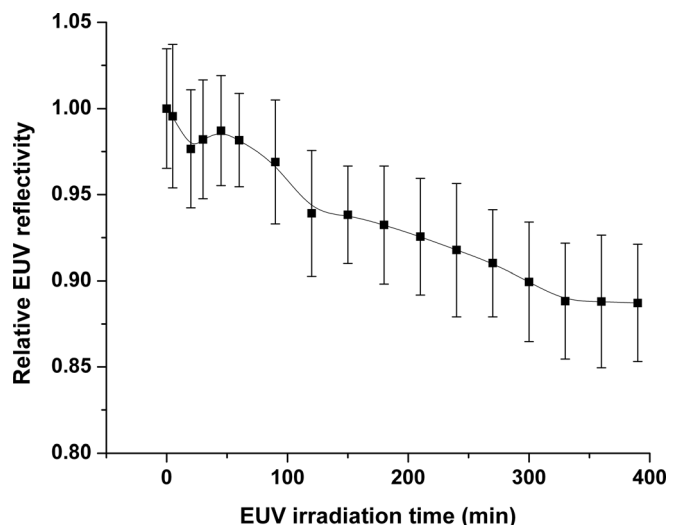


Fig. 10. Changes in Ru mirror relative EUV reflectivity vs EUR irradiation time.

#### IV. CONCLUSIONS

We investigated the change in chemical properties on the sputter cleaned Ru surface by exposing it to a 13.5 nm wavelength of EUV light radiation and its time history. The contamination of the Ru mirror surface is caused by residual impurities of the test chamber. The change in chemical composition on the Ru mirror surface was examined by *in situ* XPS to understand the modification in the corresponding EUVR when the Ru film was subjected to a continuous EUV radiation for 6 h. Detailed XPS analyses show an adsorption-mediated sudden increase in water molecules and other contaminants at the surface followed by the suppression of the Ru  $3d_{5/2}$  peak intensity by exposing the sputter cleaned Ru surface to EUV radiation. The slow decrease in H<sub>2</sub>O concentration after 30 min is discussed in terms of EUV assisted dissociation of water molecules. In addition, the rapid increase in carbon concentration up to 22% during the first hour is explained in terms of adsorption of hydrocarbons at the mirror surface, whereas a slow but linear increase in carbon concentration by suppressing the Ru  $3d_{5/2}$  peak intensity in the following hours is addressed on the grounds of accumulation of free carbon on the Ru mirror surface via dissociation of hydrocarbons. In fact, the linear reduction of the Ru  $3d_{5/2}$  peak intensity was used to estimate the thickness of the carbon layer, which was calculated to be 0.26 nm. Moreover, the variation in RuO<sub>2</sub> concentration is further discussed in view of a competition between water adsorption and dissociation in the presence of EUV radiation. All of these chemical changes were found to contribute to an ~10% decrease in EUVR of the Ru mirror after 6 h of EUV radiation at a grazing angle of ~15°. For studying carbon and related contamination issues, most of the previous studies used external hydrocarbon injection into the test chamber. Our studies showed that the impurities present in the mildly baked chamber affect the surface properties of reflecting mirrors and hence changes in EUV reflectivity with time.

#### ACKNOWLEDGMENTS

This work is partially supported by College of Engineering, Purdue University, and SEMATECH, Inc.

- <sup>1</sup>B. Wu and A. Kumar, *J. Vac. Sci. Technol. B* **25**, 1743 (2007).
- <sup>2</sup>S. A. Bajt *et al.*, *J. Microlithogr., Microfabr., Microsyst.* **5**, 023004 (2006).
- <sup>3</sup>S. Bajt, N. V. Edwards, and T. E. Madey, *Surf. Sci. Rep.* **63**, 73 (2008).
- <sup>4</sup>S. Braun, H. Mai, M. Moss, R. Scholz, and A. Leson, *Jpn. J. Appl. Phys., Part 1* **41**, 4074 (2002).
- <sup>5</sup>H. Over, Y. B. He, A. Farkas, G. Mellau, C. Korte, M. Knapp, M. Chandhok, and M. Fang, *J. Vac. Sci. Technol. B* **25**, 1123 (2007).
- <sup>6</sup>R. M. Lambert, G. Kyriakou, D. J. Davis, R. B. Grant, D. J. Watson, A. Keen, and M. S. Tikhov, *J. Phys. Chem. C* **111**, 4491 (2007).
- <sup>7</sup>G. A. Somorjai, L. Belau, J. Y. Park, T. Liang, and H. Seo, *J. Vac. Sci. Technol. B* **27**, 1919 (2009).
- <sup>8</sup>J. Hollenshead and L. Klebanoff, *J. Vac. Sci. Technol. B* **24**, 64 (2006).
- <sup>9</sup>K. Koida and M. Niibe, *Appl. Surf. Sci.* **256**, 1171 (2009).
- <sup>10</sup>J. Hollenshead and L. Klebanoff, *J. Vac. Sci. Technol. B* **24**, 118 (2006).
- <sup>11</sup>B. V. Yakshinskiy and R. A. Bartynski, *Proc. SPIE* **7636**, 76360F (2010).
- <sup>12</sup>B. V. Yakshinskiy, R. Wasielewski, E. Loginova, and T. E. Madey, *Proc. SPIE* **6517**, 65172Z (2007).
- <sup>13</sup>T. Madey, N. Faradzhev, B. Yakshinskiy, and N. Edwards, *Appl. Surf. Sci.* **253**, 1691 (2006).
- <sup>14</sup>Y. Tanaka, K. Hamamoto, H. Tsubakino, T. Watanabe, and H. Kinoshita, *Jpn. J. Appl. Phys., Part B* **44**, 5547 (2005).
- <sup>15</sup>M. Catalfano, A. Kanjilal, A. Al-Ajlony, S. S. Harilal, and A. Hassanein, *J. Appl. Phys.* **111**, 016103 (2012).
- <sup>16</sup>A. Egbert, B. Tkachenko, S. Becker, and B. N. Chichkov, *Proc. SPIE* **5448**, 693 (2004).
- <sup>17</sup>D. J. D. G. Kyriakou, R. B. Grant, D. J. Watson, A. Keen, and R. M. L. M. S. Tikhov, *J. Phys. Chem. C* **111**, 4 (2007).
- <sup>18</sup>J. Moulder, F. W. Stickle, F. P. Sobol, and K. Bomben, *Handbook of X-Ray Photoelectron Spectroscopy* (Perkin-Elmer, Eden Prairie, MN, 1992).
- <sup>19</sup>Y.-H. Lai, Y.-L. Chen, Y. Chi, C.-S. Liu, A. J. Carty, S.-M. Peng, and G.-H. Lee, *J. Mater. Chem.* **13**, 1999 (2003).
- <sup>20</sup>A. Fohlisch, N. Wassdahl, J. Hasselstrom, O. Karis, D. Menzel, N. Martensson, and A. Nilsson, *Phys. Rev. Lett.* **81**, 1730 (1998).
- <sup>21</sup>R. Schlaf, C. D. Merritt, L. C. Picciolo, and Z. H. Kafafi, *J. Appl. Phys.* **90**, 1903 (2001).
- <sup>22</sup>S. Tanuma, C. J. Powell, and D. Penn, *Surf. Interface. Anal.* **21**, 165 (1993).
- <sup>23</sup>M. Niibe, K. Koida, and Y. Kakutani, *J. Vac. Sci. Technol. B* **29**, 011030 (2011).